

## PERTURBATIONS BY MASS LOSS IN THE ORBITAL ELEMENTS OF $\gamma$ PERSEI AND $\alpha$ CENTAURI

J. F. Ling,<sup>1</sup> P. Magdalena,<sup>2</sup> and C. Prieto<sup>2</sup>

Observatorio Astronómico R. M. Aller  
Universidade de Santiago de Compostela, Spain

Received 2000 November 13; accepted 2001 June 19

### RESUMEN

Utilizando los trabajos realizados por Prieto y Docobo sobre el problema de dos cuerpos con pérdida isotrópica de masa en cada una de sus componentes, de acuerdo con la ley Eddington-Jeans, se estudia el comportamiento evolutivo de los elementos orbitales correspondientes a los sistemas binarios  $\gamma$  Persei y  $\alpha$  Centauri.

### ABSTRACT

Prieto and Docobo's approach to the two-body problem with isotropic mass loss is used to study the dynamical evolution of the orbital elements of the binaries  $\gamma$  Persei and  $\alpha$  Centauri under the assumption that mass losses obey the Eddington-Jeans law, with separate parameters for each component of the binaries.

*Key Words:* **BINARY STARS — CELESTIAL MECHANICS — STARS: MASS LOSS**

### 1. INTRODUCTION

Analytical solutions of the two-body problem for masses that vary in accordance with the Eddington-Jeans law  $\dot{m} = -\alpha m^n$  (Eddington 1924; Jeans 1924) have recently been obtained:

- a) for  $m$  as the total mass of the system (Prieto & Docobo 1997a).
- b) With separate  $\alpha$  and  $n$  for each of the two components (Prieto & Docobo 1997b).

Here we apply the solution obtained in case b) to  $\gamma$  Persei and  $\alpha$  Centauri.

### 2. METHOD

We consider a two-body system in which mass losses by the two bodies conform to the laws

$$\begin{aligned} \dot{m}_1 &= -\alpha m_1^n, \\ \dot{m}_2 &= -\beta m_2^p. \end{aligned} \tag{1}$$

The Hamiltonian function is

$$F = -\frac{1}{2} \frac{m_1^2 + m_2^2 + 2m_1m_2}{L^2} + \frac{\dot{m}_1 + \dot{m}_2}{m_1 + m_2} L e \sin E. \tag{2}$$

<sup>1</sup>Member of Dpto. Matemática Aplicada, Universidade de Santiago de Compostela, Spain.

<sup>2</sup>Members of Dpto. Matemática Aplicada, Universidade de Vigo, Spain.

and the equations of motion

$$\begin{aligned} \frac{d\ell}{dt} &= \frac{\partial F}{\partial L}; & \frac{dg}{dt} &= \frac{\partial F}{\partial G} \\ \frac{dL}{dt} &= -\frac{\partial F}{\partial \ell}; & \frac{dG}{dt} &= -\frac{\partial F}{\partial g} = 0. \end{aligned} \quad (3)$$

where  $L, G, \ell$ , and  $g$  are the Dalaunay variables (Prieto & Docobo 1997a). On expanding  $m_1(t)$  and  $m_2(t)$  as Taylor series in the neighbourhood of an initial time  $t = t_0$  the Hamiltonian can be written in powers of two small parameters  $\epsilon_1$  and  $\epsilon_2$  (the dimensionless equivalents of  $\alpha$  and  $\beta$ ); this series can be truncated at any desired order, and the resulting equations of motion can then be integrated analytically; specifically, a method based on Lie transformations is used to obtain a generating function  $W = \epsilon_1 W^1 + \epsilon_2 W^2$  affording the canonical transformation from the variable set  $(L, G, \ell, g)$  to another, more manageable, set  $(L^*, G^*, \ell^*, g^*)$ .  $L^*, G^*, g^*$  are constants and  $\ell^*$  is quadratic in  $t$ .

For our present purposes it suffices to expand the Hamiltonian up to first order in  $\epsilon_1$  and  $\epsilon_2$  because the terms of higher order are negligible (Prieto & Docobo 1997b). We therefore write

$$\begin{aligned} F &= F_0 + \epsilon_2 F_{01} + \epsilon_1 F_{10} = -\frac{(m_{10} + m_{20})^2}{2L^2} + \\ &+ \epsilon_1 \left[ \frac{(m_{10}^{n+1} + m_{10}^n m_{20})}{L^2} (t - t_0) - \frac{L e m_{10}^n \sin E}{m_{10} + m_{20}} \right] \\ &+ \epsilon_2 \left[ \frac{(m_{20}^{p+1} + m_{20}^p m_{10})}{L^2} (t - t_0) - \frac{L e m_{20}^p \sin E}{m_{10} + m_{20}} \right] \end{aligned} \quad (4)$$

where  $m_{10}, m_{20}$  are the values of  $m_1$  and  $m_2$  in the initial instant  $t_0$ .

Under these conditions and with the equations of the biparametric method (Prieto & Docobo 1997b) we can obtain  $W^1$  and  $W^2$

$$\begin{aligned} W^1 &= \frac{L^{*4} e^* m_{10}^n \cos E^*}{(m_{10} + m_{20})^3} \left( 1 - \frac{e^* \cos E^*}{2} \right), \\ W^2 &= \frac{L^{*4} e^* m_{20}^p \cos E^*}{(m_{10} + m_{20})^3} \left( 1 - \frac{e^* \cos E^*}{2} \right). \end{aligned} \quad (5)$$

For given values  $m_{10}, m_{20}, P_0, T_0, e_0, a_0$ , and  $\omega_0$  of the masses and orbital elements of the system at time  $t_0$  the solution is unique and can be used to calculate  $(L^*, G^*, \ell^*, g^*)$  for any time  $t$ . The variables  $(L, G, \ell, g)$  are then given by

$$\begin{aligned} L &= L^* - \frac{\partial W}{\partial \ell^*}, \\ G &= G^* - \frac{\partial W}{\partial g^*}, \\ \ell &= \ell^* + \frac{\partial W}{\partial L^*}, \\ g &= g^* + \frac{\partial W}{\partial G^*}, \end{aligned} \quad (6)$$

and the equation for  $\ell^*$  is

$$\ell^* = A^*_0 + A^*_1 t + A^*_2 t^2, \quad (7)$$

where

$$A^*_1 = \frac{(m_{10} + m_{20})^2 + 2(m_{10} + m_{20})t_0(\epsilon_1 m_{10}^n + \epsilon_2 m_{20}^p)}{L^{*3}},$$

$$A^*_2 = -\frac{(m_{10} + m_{20})(\epsilon_1 m_{10}^{n+1} + \epsilon_2 m_{20}^p m_{10})}{m_{10} L^{*3}},$$
(8)

and  $A^*_0$  is an integration constant. Finally, the orbital elements follow

$$P = 2\pi\sqrt{\frac{a^3}{m}},$$

$$T = t - \frac{l}{2\pi}\sqrt{\frac{m}{a^3}},$$

$$e = \sqrt{1 - \frac{G^2}{L^2}},$$

$$a = \frac{L^2}{m},$$

$$\omega = g,$$
(9)

$m$  being the total mass of the system.

### 3. APPLICATIONS

We have applied the above approach to the well-known binary stars,  $\gamma$  Persei and  $\alpha$  Centauri. There is abundant physical and dynamical information for these stars (in particular, the masses of their components are known with great precision because both are spectro-interferometric binaries), but they differ widely in their characteristics,  $\gamma$  Persei comprising a G giant and an early A star on the main sequence, and  $\alpha$  Centauri two components of solar type.

#### 3.1. $\gamma$ Persei

$\gamma$  Persei (WDS 03048+5330, HD 18925, HIP 14328) is a spectro-interferometric and photometric double star for which visual orbits have been published by McAlister (1982), Popper & McAlister (1987), and Pourboix (1999). The most reliable orbital elements are those of Pourboix, which were accordingly used as the initial values of the orbital elements in this work (Table 1). The initial masses of each component listed in Table 1 were calculated using Pourboix's orbit and a spectroscopic orbit also published by Popper & McAlister (1987). Physical parameters calculated using Allende & Lambert's (1999) procedure are shown in Table 2 together with the trigonometric parallax  $\pi$  given by *Hipparcos* (ESA 1997).

As mass loss laws we used:

$$m_1 = -1.0617 \times 10^{-9} m_1^{3.5},$$

$$m_2 = -1.4701 \times 10^{-11} m_2^4,$$
(10)

where  $m_1$  and  $m_2$  are the masses of the A and the B component, respectively.

The values of  $\alpha$  and  $\beta$  of equation (1) were obtained from the relation

$$\log(-\dot{M}) = -1.01 + 1.96 \log\left(\frac{L}{L_\odot}\right) - 3.54 \log(T_{eff}).$$
(11)

This relation is based on Waldron's empirical correlations (Waldron 1985), which are valid for stars for which, as in the case of  $\gamma$  Persei,

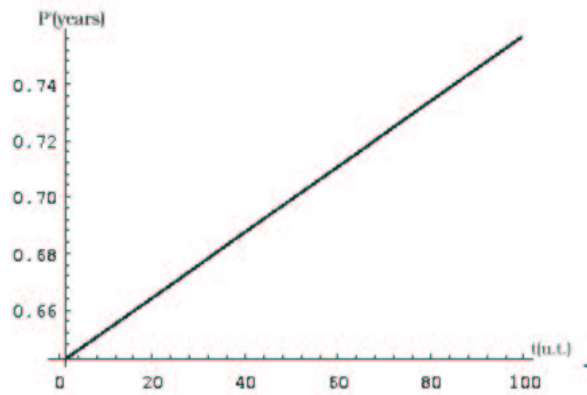


Fig. 1. Variation of perturbed period,  $P$ . For a better visualization we plot the quantity  $P'=(P-14.7651)\times 10^4$  on the y-axis.

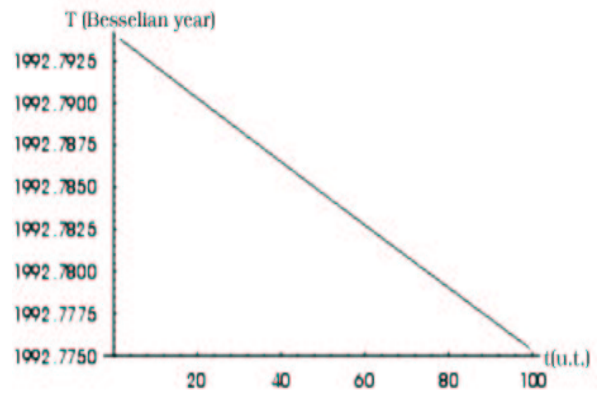


Fig. 2. Variation of perturbed time of periastron passage,  $T$ .

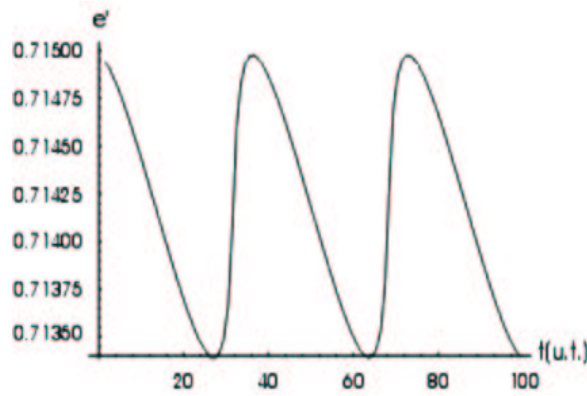


Fig. 3. Variation of perturbed eccentricity,  $e$ . For a better visualization we plot the quantity  $e'=(e-0.7849999)\times 10^8$  on the y-axis.

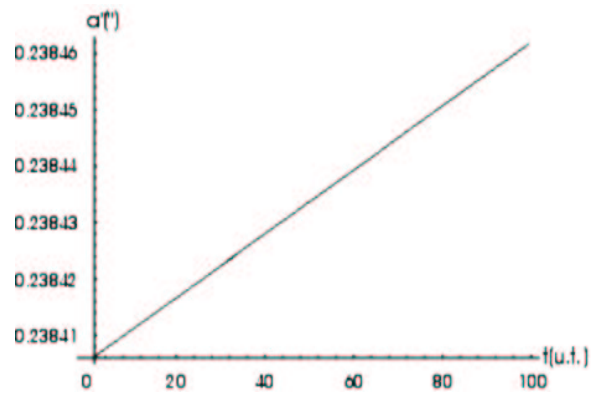


Fig. 4. Variation of perturbed semimajor axis,  $a$ . For a better visualization we plot the quantity  $a'=(a-0.144)\times 10^4$  on the y-axis.

TABLE 1

ORBITAL ELEMENTS AND MASSES  
( $\gamma$  PERSEI)

$P_0$ (years)	=	14.6
$T_0$ (Besselian year)	=	1991.08
$e_0$	=	0.785
$a_0$ (")	=	0.144
$i_0$ ( $^\circ$ )	=	90.9
$\Omega_0$ ( $^\circ$ )	=	244.1
$\omega_0$ ( $^\circ$ )	=	170.0
mass A ( $M_\odot$ )	=	2.7
mass B ( $M_\odot$ )	=	1.65

TABLE 2

PHYSICAL PARAMETERS ( $\gamma$  PERSEI)

	A Star	B Star
Spectral Type	G8III	A3V
Absolute Magnitude	-1.23	0.01
$T_{eff}$ ( $^\circ$ K)	4885	7895
$L(L_\odot)$	97.724	288.403
$\pi$ ( <i>Hipparcos</i> )	0''01272	

TABLE 3

ORBITAL ELEMENTS AND MASSES  
( $\alpha$  CENTAURI)

$P_0$ (years)	=	79.9
$T_0$ (Besselian year)	=	1955.59
$e_0$	=	0.519
$a_0$ (")	=	17.59
$i_0$ ( $^\circ$ )	=	79.23
$\Omega_0$ ( $^\circ$ )	=	204.82
$\omega_0$ ( $^\circ$ )	=	231.8
mass A ( $M_\odot$ )	=	1.16
mass B ( $M_\odot$ )	=	0.97

TABLE 4

PHYSICAL PARAMETERS ( $\alpha$  CENTAURI)

	A Star	B Star
Spectral Type	G2V	K1V
Absolute Magnitude	4.327	5.667
$T_{eff}$ ( $^\circ$ K)	5830	5255
$L(L_\odot)$	1.532	2.021
$\pi$ ( <i>Hipparcos</i> )	0''74212	

$$3.2 \leq \log(T_{eff}) \leq 4.8,$$

and

$$2.0 \leq \log\left(\frac{L}{L_\odot}\right) \leq 6.5,$$

(Valls-Gabaud 1988). The exponents  $n$  and  $p$  were obtained by interpolation of the data in Eddington's Table I (Eddington 1924), which Eddington calculated using the empirical expression

$$L = c m^{7/5} (1 - b)^{3/2} 2.11^{4/5} T_{eff}^{4/5}, \tag{12}$$

where  $(1 - b) = 0.00309 m^2 2.11^4 b^4$  and  $c$  is an observational constant.

With the above initial values and parameters, the method sketched in the previous section was used to calculate the time-dependence of the orbital elements over 100,000 years. Figures 1 to 5 show the evolution of the orbital elements over the last 100 time units which would correspond to about 150 years (see figure captions for the scaling of the y-axes).

### 3.2. $\alpha$ Centauri

Orbits for our nearest double star (WDS 14396-6050, HD 128620, HIP 71683) have been calculated by Finsen (1926), Wielen (1962), Heintz (1982), and Purboix, Neuforge-Verheecke, & Noels (1999). For the initial

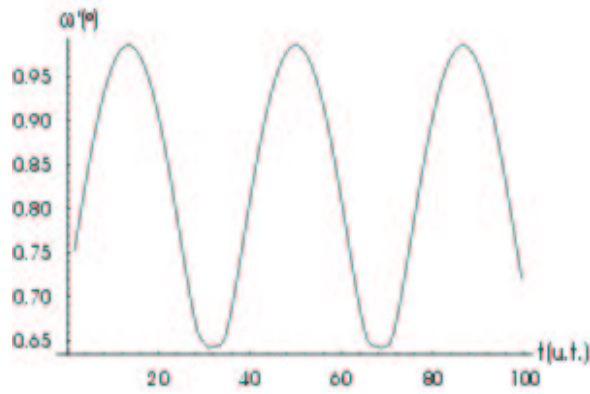


Fig. 5. Variation of perturbed longitude of periastron,  $\omega$ . For a better visualization, we plot the quantity  $\omega'=(\omega-169.99999999) \times 10^{10}$  on the y-axis.

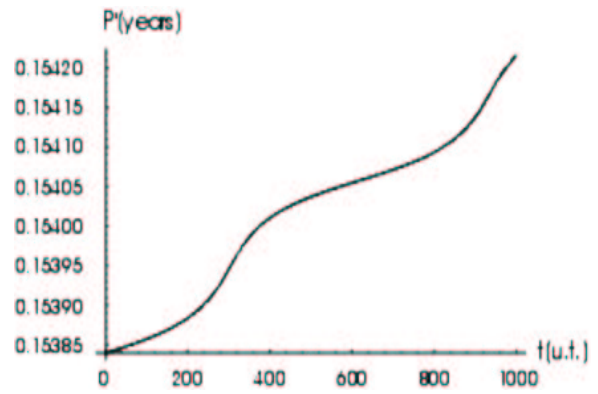


Fig. 6. Variation of perturbed period,  $P$ . For a better visualization we plot the quantity  $P'=(P-79.9) \times 10^6$  on the y-axis.

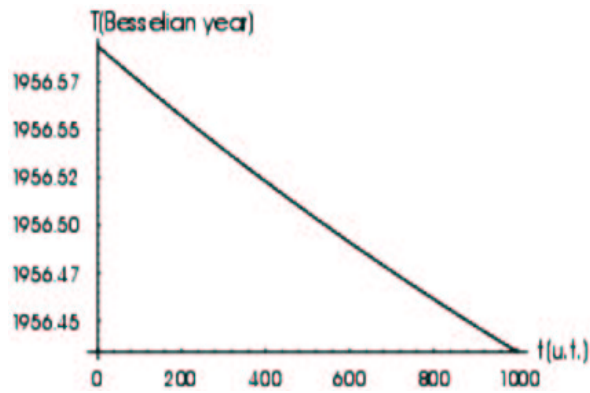


Fig. 7. Variation of perturbed time of periastron passage,  $T$ .

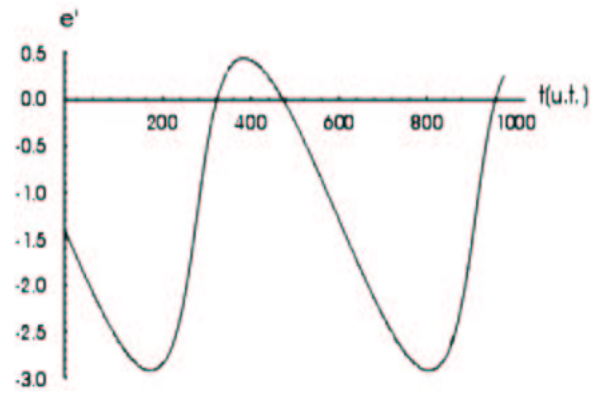


Fig. 8. Variation of perturbed eccentricity,  $e$ . For a better visualization we plot the quantity  $e'=(e-0.519) \times 10^{13}$  on the y-axis.

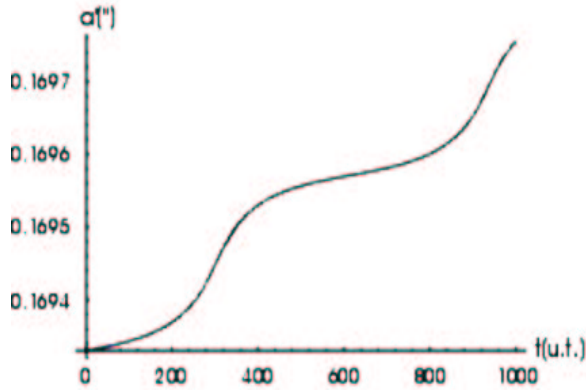


Fig. 9. Variation of perturbed semimajor axis,  $a$ . For a better visualization we plot the quantity  $a'=(a-17.59)\times 10^7$  on the y-axis.

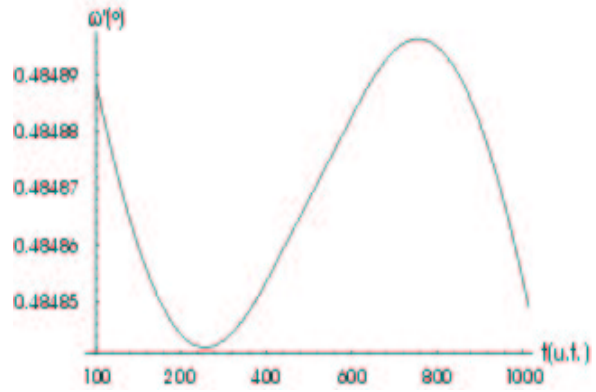


Fig. 10. Variation of perturbed longitude of periastron,  $\omega$ . For a better visualization we plot the quantity  $\omega'=(\omega-231.799999)\times 10^7$  on the y-axis.

values of the orbital elements we have again used Pourboix et al.'s solution, which is based on visual and spectroscopic data and exhibits best overall fit to the complete set of observations; these elements are listed in Table 3 together with the corresponding initial masses. Physical parameters published by Neuforge-Verheucke & Magain (1997) are listed in Table 4 together with the *Hipparcos* parallax.

The mass loss laws considered in this case were:

$$\begin{aligned} \dot{m}_1 &= -0.350141 \times 10^{-14} m_1^4, \\ \dot{m}_2 &= -0.350141 \times 10^{-14} m_2^{2.7}, \end{aligned} \tag{13}$$

where the values of  $\alpha$  and  $\beta$  are both equal to the value corresponding to solar mass loss (Schatzman & Praderie 1993), but the exponents  $n$  and  $p$  were obtained in the same way as for  $\gamma$  Persei. As for  $\gamma$  Persei, calculations were carried out for a 100,000 year time interval, but since the orbital period of  $\alpha$  Centauri is greater than that of  $\gamma$  Persei, we show in Figures 6 to 10 the variation of the elements over the last 1000 time units, corresponding to about 1300 years (see figure captions for the scaling of the y-axes).

#### 4. CONCLUSIONS

In spite of the wide physical and dynamical differences between  $\gamma$  Persei and  $\alpha$  Centauri, the overall behaviour of their orbital elements is similar: the period, semiaxis major, and periastron epoch exhibit secular behaviour (these trends continue throughout the 100,000 year interval studied) while the eccentricity and the argument of periastron vary periodically (some periodic variation is also superimposed on the linear trends of the period and semiaxis major of  $\alpha$  Centauri). In all cases, however, the rates of variation are very small especially in the case of  $\alpha$  Centauri which has the smaller mass loss.

All these calculations were carried out on a FUJITSU vectorial computer model VPP300 in the Supercomputation Center of Galicia (CESGA).

We wish to thank C. Allende for data supplied to us. This work was supported by the Xunta de Galicia (Spain) under project PGIDT-99-PX-124301B.

#### REFERENCES

Allende, C., & Lambert, D. L. 1999. *A&A*, 352, 555

- Eddington, A. S. 1924, MNRAS, 84, 308  
ESA 1997, The *Hipparcos* and *Tycho* Catalogues, (Noordwijk, The Netherlands: ESA Pub. Div. ESTEC)  
Finsen, W. S. 1926, Union. Obs. Cir., 63, 343  
Heintz, W. D. 1982, The Observatory, 102, 42  
Jeans, J. H. 1924. MNRAS, 85, 1  
McAlister, H. A. 1982, AJ, 87, 563  
Neuforge-Verheecke, C., & Magain, P. 1997, A&A, 328, 261  
Pourboix, D. 1999, A&A, 348, 127  
Pourboix, D., Neuforge-Verheecke, C., & Noels, A. 1999, A&A, 344, 172  
Popper, D. M., & McAlister, H. A. 1987, AJ, 94, 700  
Prieto, C., & Docobo, J. A. 1997a, A&A, 318, 657  
\_\_\_\_\_. 1997b, Cel. Mech. & Dyn. Astron., 68, 53  
Schatzman, E. L., & Praderie, F. 1993, The Stars (Berlin: Springer-Verlag)  
Valls-Gabaud, D. 1988, Ap&SS, 142, 289  
Waldron, W. L. 1985, in The Origin of Non-Radiative Heating/Momentum in Hot Stars, eds. A. B. Underhill & A. G. Michalitsianos, NASA CP-2358, 95  
Wielen, R. 1962, AJ, 67, 599